Journal of Engineering and Applied Sciences 13 (17): 7450-7458, 2018
ISSN: 1816-949X

Tunable Notch Fiber Bragg Grating Optical Filter

Aia T. Yhia, Tahreer S. Mansour and Yousif I. Hammadi
Institute of Laser for Postgraduate Studies, University of Baghdad, Baghdad, Iraq

Abstract: This study presents a continuously tunable optical notch filter based on homodyne Machzehnder interferometer (Machzehnder using dual uniform fiber Bragg gratings) is proposed. The tunability of the filter is achieved by wavelength tuning of the fiber Bragg gratings to adjust the basic time delay provided by a dispersive element. Tunability of the filter can be generated by applying mechanical and physical effects which are strain and force on the second arm of homodyne Mach-Zehnder interferometer, i.e., (effected arm). It has been shown from the results that the FBG is very sensitive to variations in strain over a range of (0-0.31) and the normalized sensitivity from 62.8758-62.8743, shifted Bragg wavelength from 1545.726-1545.764 nm, full width at half maximum from 197.529-238.080 pm and power from 12.1-11 nW and in the theoretical optiwave, obtained to the shifted Bragg wavelength from 1454.766-1546.25 nm. It observed that when tensile strain applied to the second arm of homodyne MZI, showed shifting in center wavelength (red shift). Also, observed from the results, the relation between the shifted Bragg wavelength and micro strain is nonlinear.

Key words: Fiber-optic sensors, Mach-Zehnder Interferometer (MZI), Fiber Bragg Grating (FBG), strain and force measurements, Bragg wavelength, tensile

INTRODUCTION

Optical fiber dual Brag gratings Mach-Zehnder Interferometer (MZI) have attracted a lot of interest for various physical and mechanical effected applications due to their simple structure, capability of responding to a variety of measurands, ease of fabrication and low cost (Meera and Anuradha, 2014). Homodyne MZI has two Fibers Bragg Grating (FBG) arms, one used as effected arm and another used as reference arm, the effected arm is exposed to external variations such as temperature, refractive index, strain, etc. while reference arm is kept isolated from variations (Allsop *et al*., 2002). Combined output at the MZI output coupler port has the interference component according to the optical phase difference between two arms, the change induced in the effected arm by any of the measurands changes the optical phase difference of the MZI which can be easily detected by analyzing the variation in the interference spatially and temporally signal (Lee *et al*., 2012). Optical fiber Bragg gratings are important components in fiber communication and fiber sensing fields. For normal fiber Bragg gratings by properly choosing the period, length, index modulation amplitude, chirp and apodization function, one can flexibly design and optimize grating reflection or transmission spectra to satisfy many applications (Anonymous, 2003). Although, optical fibers have been used for many decades, the last 10-20 years have shown a lot of further development. The FBGs are used extensively in telecommunication industry for dense wavelength division multiplexing, dispersion compensation laser stabilization and Erbium amplifier gain flattening, simultaneous compensation of fiber dispersion, dispersion slope and optical CDMA (Tan *et al*., 2009; Navruz and Guler, 2008). By exploiting the characteristics exhibited by these gratings, numerous areas have been marked in which their usage has brought drastic advancements and continues to do the same. The FBG works on the principle that when Ultraviolet Light (UV) illuminates a certain kind of optical fiber, the refractive index of the fiber is changed permanently, this effect is called photosensitivity. Alternatively, the refractive index will last for several years if it is followed by proper annealing (Wu *et al*., 2005). This technique uses the interference pattern of ultraviolet laser light to create the periodic structure of FBGs. Since, this discovery, the development in the field of Bragg gratings has experienced a tremendous growth. FBGs offer ample advantages but the most important is the flexibility in spectral characteristics. Many researchers have been work done in this field also (Mizunami *et al*., 2000).

Theoretical overview: The schematic diagram of a Mach-zehnder interferometer is shown in Fig. 1. It consist of two coupler at the input and the output and two fiber Bragg grating the first one called reference arm and the second called effected arm. When applied tensile strain on the second arm of homodyne MZI, resulting optical path difference between the reference and effected fibers. The light intensity of the output of MZI can be expressed as (Jackson *et al*., 1982):

Corresponding Author: Aia T. Yhia, Institute of Laser for Postgraduate Studies, University of Baghdad, Baghdad, Iraq

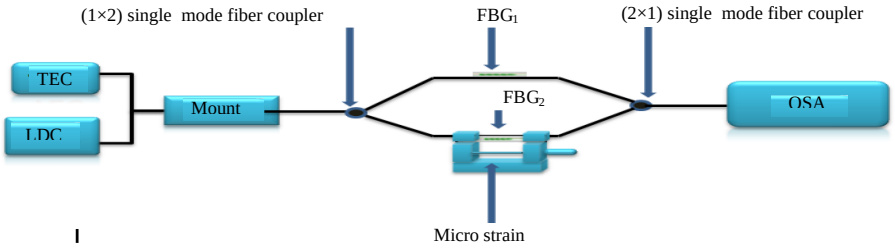

Fig. 1: Schematic diagram of tunable optical fiber Bragg grating notch filter

$$I/I_{\circ} = 1+BCos\ [\Delta\varphi B+\Phi(t)] \quad (1)$$

Where:
I = The intensity of the incident light
B = Visibility of the interference signal
Φ(t) = The thermally induced phase drift in the SI

The SI acts as a wavelength scanner for FBGs when the optical path of the SI is modulated. The strain-induced change in the reflected wavelength from a FBG produces a change in the optical phase $\Delta\varphi_B$ (Jackson *et al*., 1982):

$$\Delta\varphi_B = 2\pi\Delta L_{SI}\Delta\lambda_B/\lambda_B^2 = 2\pi\Delta L\zeta_g\Delta Y/\lambda_B \quad (2)$$

Where:
ΔY = The variation in strain applied to the FBG
ΔL_{SI} = The Optical Path Difference (OPD) of scanned interferometer (SI)

ζg is the normalized FBG sensitivity for strain which is given by (Jackson *et al*., 1982):

$$\zeta_g = 1/(\lambda_B)\left(\frac{\Delta\lambda_B}{\Delta Y}\right) \quad (3)$$

Hence, the phase sensitivity in response to strain ($\Delta\varphi_B/\Delta Y$) is directly proportional to the OPD in the SI. A Fiber Bragg Grating (FBG) is a wavelength selective filter, generally inscribed in the core of a fiber. The filter typically consists of a weak periodic variation of the refractive index with a periodicity given by Chung *et al*. (2012):

$$\lambda_B = 2neff\Lambda \quad (4)$$

Where:
neff = The effective refractive index and it is equal to 1.451800232
Λ = The periodicity
λ_B = The reflected wavelength

MATERIALS AND METHODS

Experiments and setup assembly

Theoretical optiwave: Figure 2 shows the simulation setup of the system utilizing OptiSystem Software.

Table 1: Wight light source have specifications

Wavelength (nm)	Frequency (THz)	Power (dBm)
1545.684	193.955	-130

The system consist of wight light source, single mode fiber with length equal (1 m), power splitter (1×2), Dual FBG, power combiner (2×1), single mode fiber (1 m) and Optical Spectrum Analyzer (OSA) (Table 1). At these specifications the interferometers shown in Fig. 3-7.

B-practical setup: The main objective is to build homodyne MZI consist of: SLD, single mode fiber coupler, FBG, OSA and PC screen. Figure 8 and 9 are photographic images of the experimental parts. It comprises of Super Luminescent Diode (SLD) source, (1×2) input single mode fiber coupler acts as splitter, dual Fiber Bragg Grating (FBG1 and FBG2) effect and reference arms respectively of homodyne Mach-zehnder interferometer, (2×1) output single mode fiber coupler acts as combiner and Optical Spectrum Analyzer (OSA) to visualize phase shift in the spectrum of the source by applied micro strain and force respectively on the second arm of homodyne MZI. Each part will be explained in brief. The light source that was used in this experiment is the Super Luminescent Diode (SLD) (THORLABS Inc.) with a spectrum range (1450-1650) nm and output power of 31.2 mW with a near Gaussian spectral profile and low ripple. The light source consists of four parts: IC Chipset, Laser Mount, Temperature Controller (TED200C) and Laser Diode Controller (LDC210C) (both TED and LDC are from THORLABS Inc.). IC Chipset (Covega Company) is the main part of the SLD from which the signal is transmitted. It involves 14 pins and it is fixed on LM14S2 Universal 14-pin Butterfly Laser Diode Mount. IC Chipset is protected from overheating by heat sink on the laser mount (Thorlabs Inc.). TED is connected to the laser mount and it is used for wavelength stabilization and also can be used for tuning of the wavelength by control its temperature in this experiment the value of temperature is equal to 16.522°C, LDC is also connected to the laser mount and it is used to control the driving current (I = 300.32 mA),

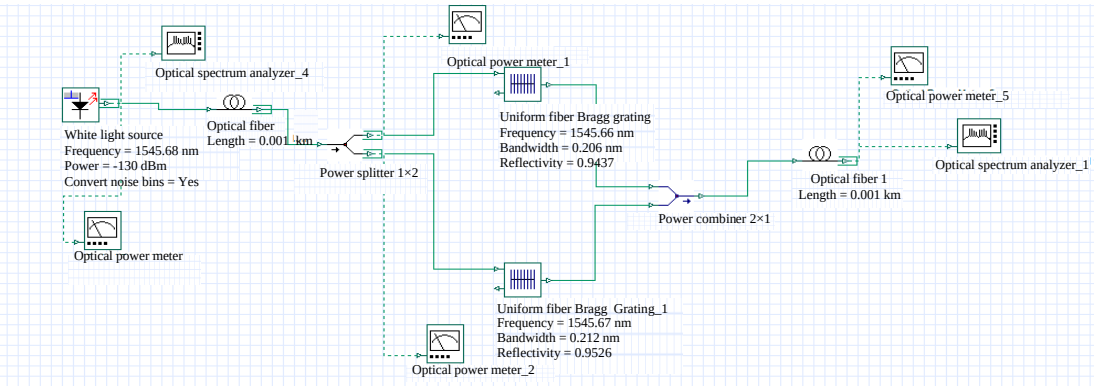

Fig. 2: The designed model of simulated system with optisystem software

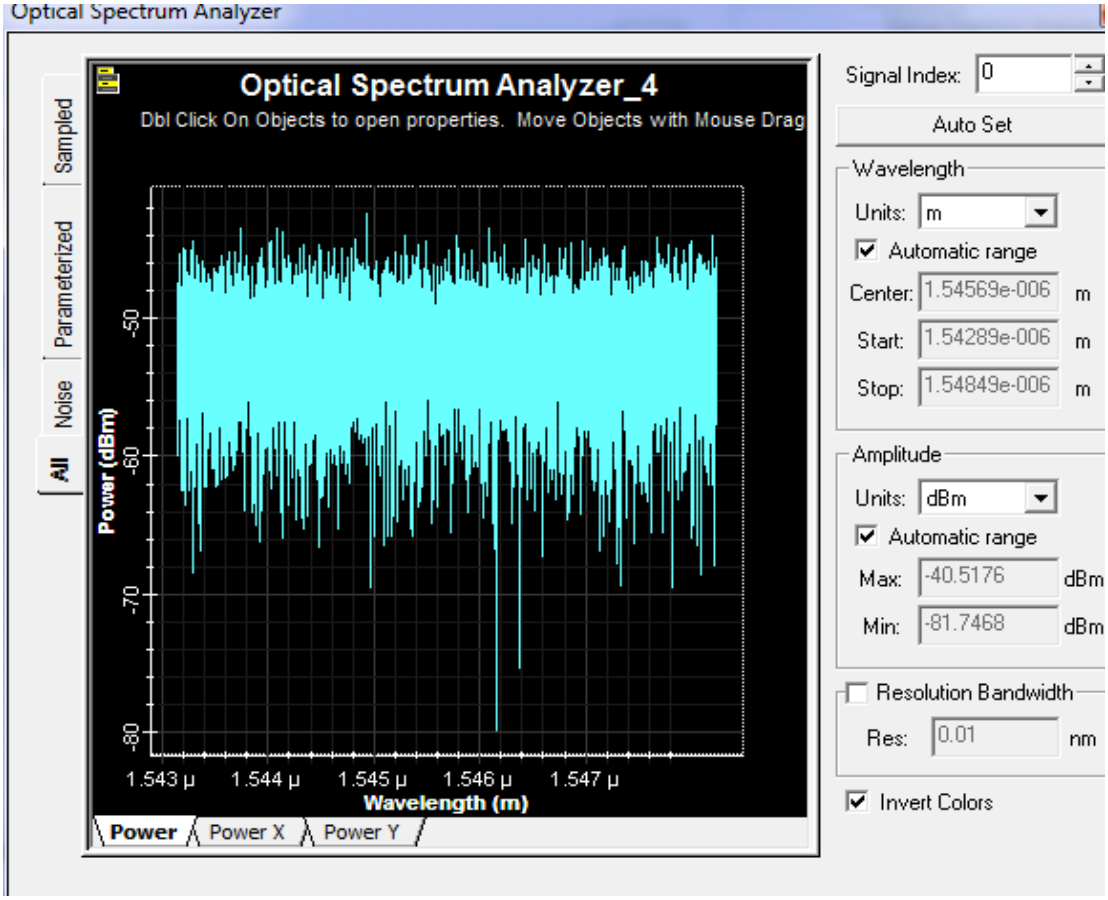

Fig. 3: Signal of wight light source

(1×2) input single mode fiber coupler acts as splitter, it have wavelength equal to (1310/1550 nm) and insertion loss = 5.0/5.0 dB, dual fiber Bragg grating (FBG1 and FBG2) where FBG1 have wavelength (1545.655 nm), grating length (10 mm), Band width (0.206 nm) and reflectivity (94.37%), FBG2 have wave length (1545.670 nm), grating length (10 mm), band width (0.212 nm) and reflectivity (95.26%), (2×1) output single mode fiber coupler acts as combiner have wavelength (1310/1550 nm) and insertion loss (0.20/0.21 dB), Optical Spectrum Analyzer (OSA) with range wavelength (600-1700 nm) and power (20 mW/13 dB max) and see results to PC screen.

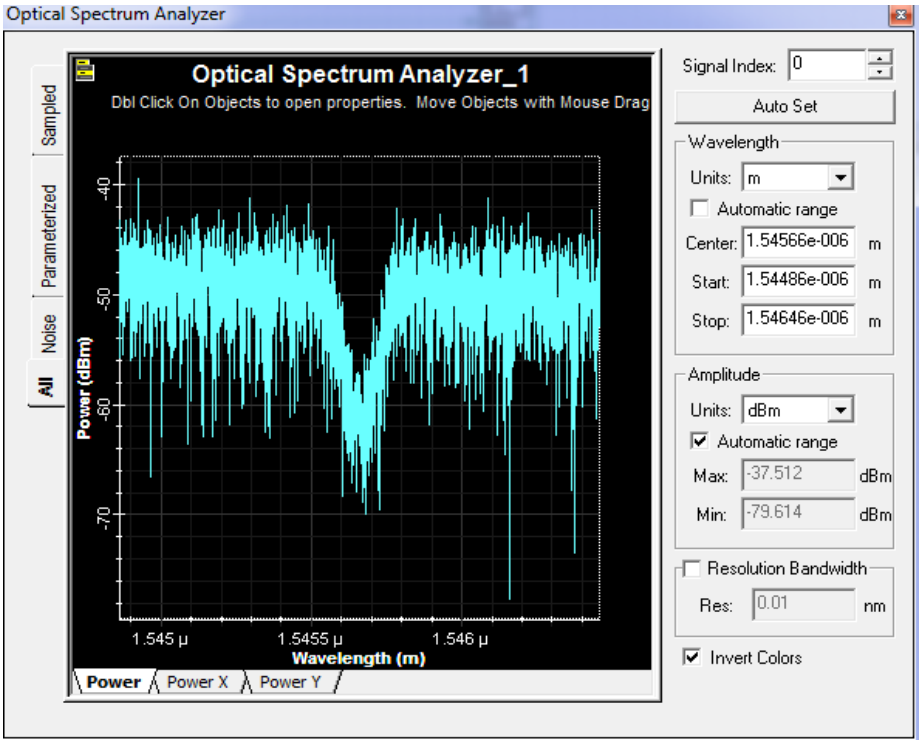

Fig. 4: Signal when applied zero strain

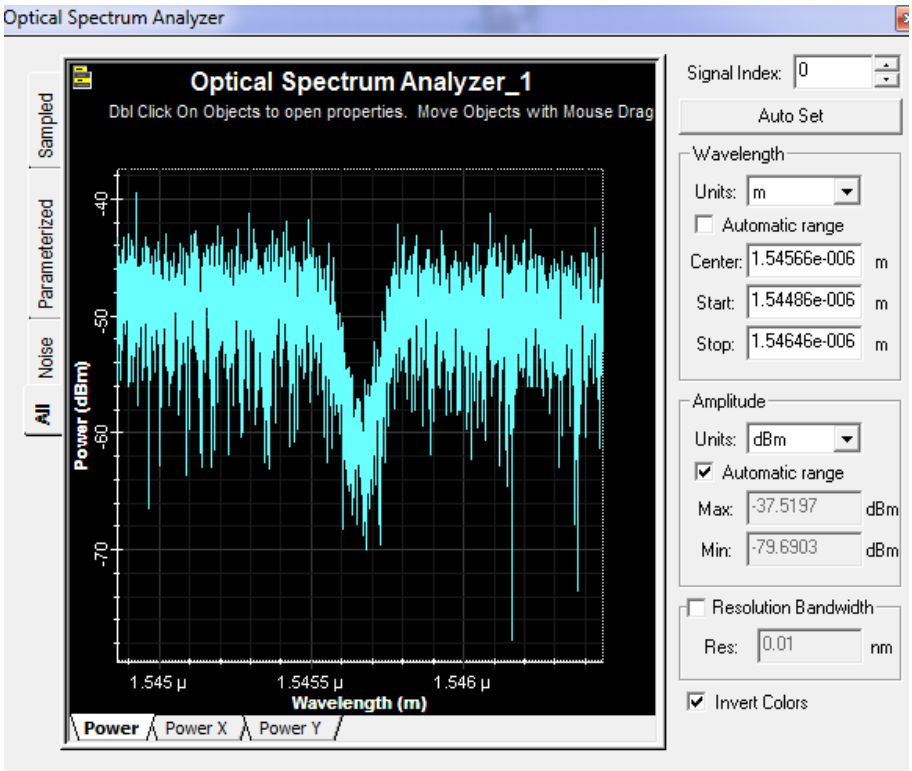

Fig. 5: At strain = 0.09 mm

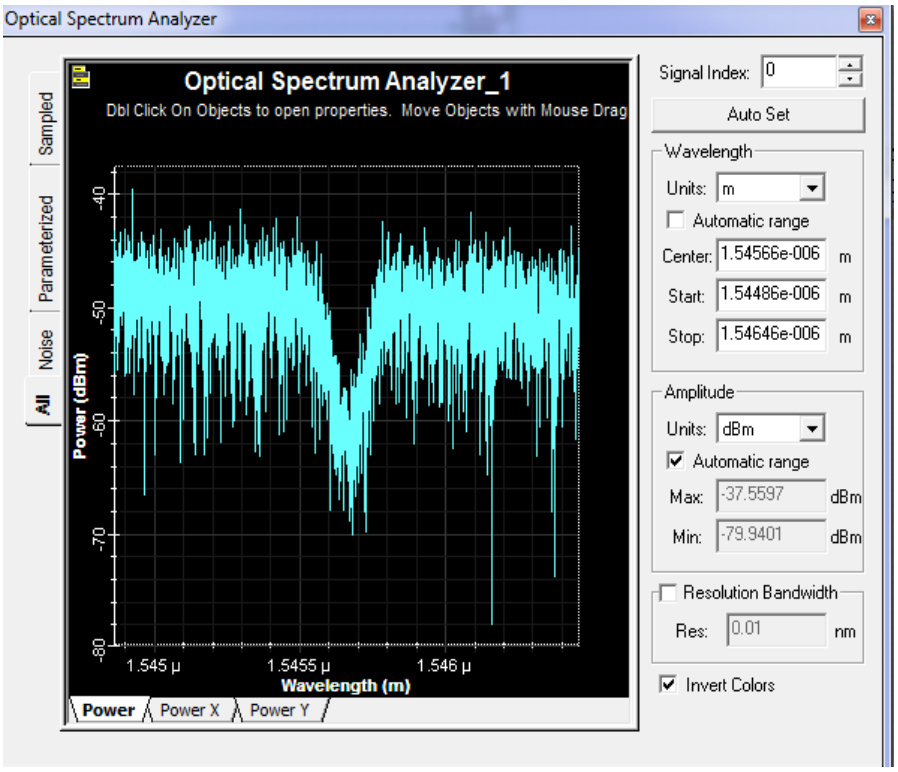

Fig. 6: At strain = 0.24 mm

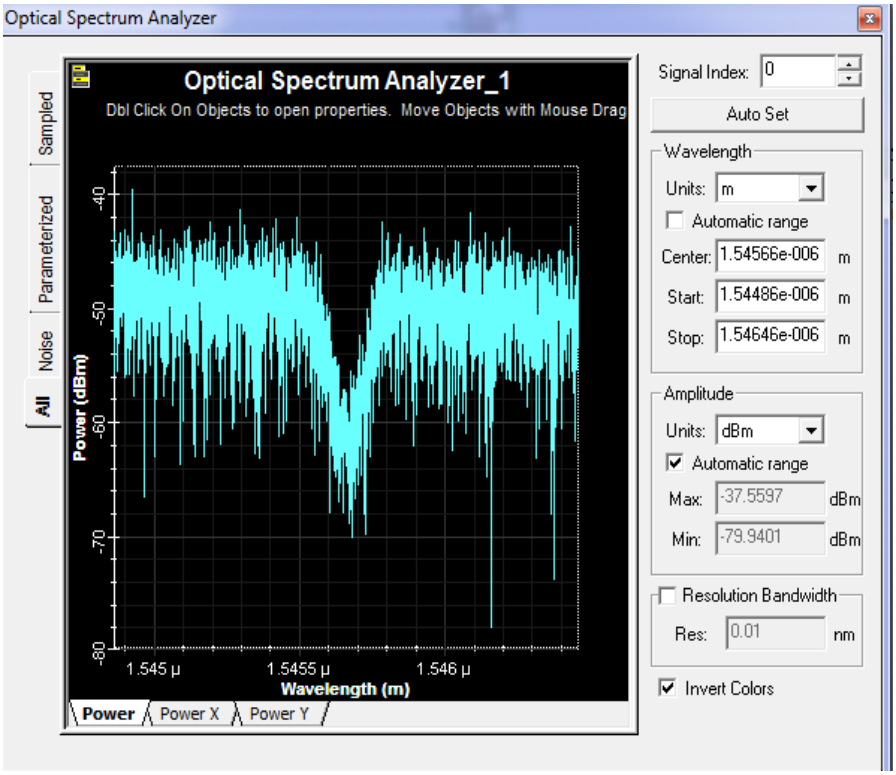

Fig. 7: At strain = 0.31 mm

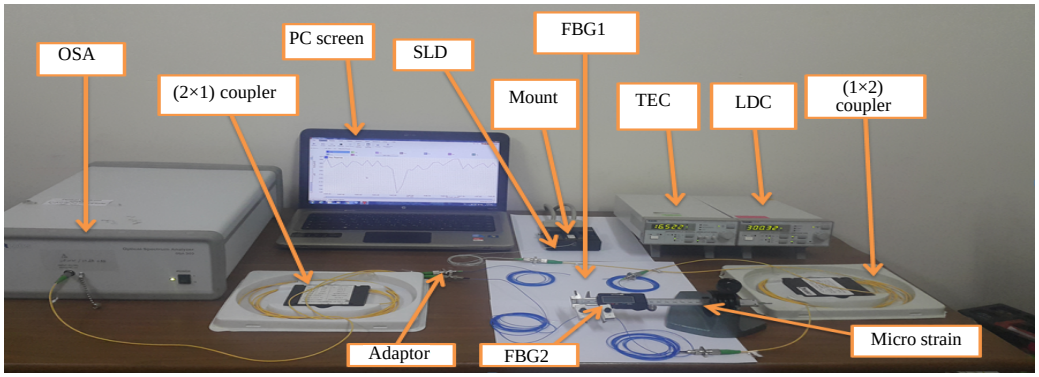

Fig. 8: A photographic image for the experimental setup when applied micro strain on the effected arm

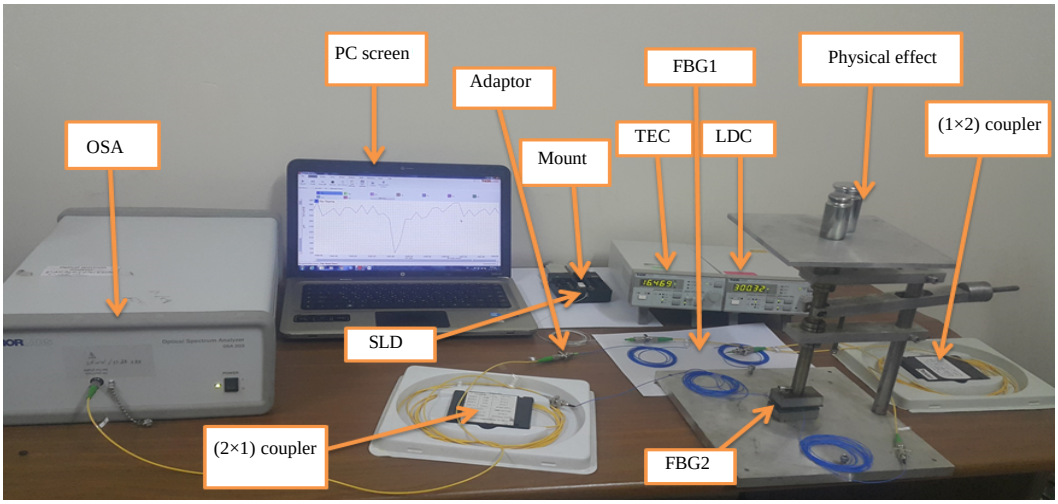

Fig. 9: A photographic image for the experimental setup when applied force on the effected arm

RESULTS AND DISCUSSION

In this research, we implemented a tunable optical notch FBG filter based on homodyne MZI practically and theoretically by OptiWave Software (Fig. 10 and 11). In practically when we are applied tensile strain on the second arm of homodyne MZI, the central wavelength (λ_B) is shifted to red shift as Fig. 12. This shifting is duo to changing in elasto-optic effected and elasticity of the fiber, causing change in neff and Λ that affects Bragg wavelength λ_B. The effected of tensile strain on the λ_B is listed in Table 2:

From Table 2, it can be seen that when there is no strain, i.e., (zero strain) is applied the λ_B = 1545.726 nm, FWHM = 197.529 pm and power = 12.1 nW when strain is applied with 0.09, λ_B = 1545.736 nm, FWHM = 216.389 pm and power =11.9 nW, and when applied strain with values (0.24 and 0.31) we can be seen that the λ_B, FWHM are increased and power is decreased, so, we can be

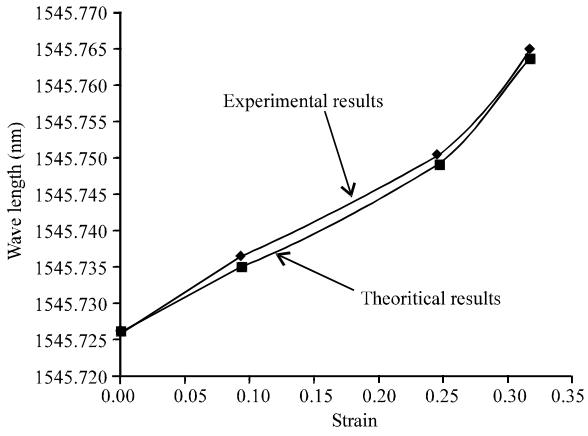

Fig. 10: Comparison between the theoretical and experiment results via. stretching technique

discussion results in generally when we applied strain on the second arm of homodyne MZI when this strain is

increased leads to λ_B and FWHM are increased but power is decreased. So, the relation between the shifted Bragg wavelength λ_B and micro strain is nonlinear. When we applied strain to the second arm of homodyne MZI lead to the period grating will be change according to Eq. 4, this change in period grating shown in Table 3 and 4.

From the Fig. 13 when applied physical effect which is force effect on the second arm of homodyne MZI, it observed that the central wavelength λ_B shifted to red shift and FWHM is increased when the power decrease, as shown in Table 5-7.

In theoretically by Optiwave Software, we obtained red shifted in Bragg wavelength from 1545.766-1546.25 nm, we obtained little different between theoretical and practical results due to temperature in the laboratory. The optical fibers are very sensitive to temperature, it's cause change in the refractive index of the fibers where the refractive index is a function of the wavelength.

Table 3: The results obtained from Opti wave shown Table 1

Strain	λB (nm)	Power (dBm)
0.00	1545.766	-64.9933
0.09	1545.971	-52.9777
0.24	1546.21	-47.2827
0.31	1546.25	-50.0004

Table 4: Tensile strain effected on the Bragg wave length (λ_B), Full Width at Half Maximum (FWHM) and power

Micro strain	Bragg wave length (nm)	FWHM (pm)	Power (nW)
0.00	1545.726	197.529	12.1
0.09	1545.736	216.389	11.9
0.24	1545.750	233.607	11.2
0.31	1545.764	238.081	11.0

Table 5: Bragg wavelengths for applied many value of strain on the second arm of MZI

Strain	Period grating (Λ) (nm)	Bragg wave length (nm)
0.00	532.348	1545.726
0.09	532.351	1545.736
0.24	532.356	1545.750
0.31	532.361	1545.764

Table 6: Comparison between the theoretical and experiment results via. stretching technique

Strain	Theoretical results of center wave length λ (nm)	Experimental results of center wave length (nm)
0.00	1545.725	1545.726
0.09	1545.734	1545.736
0.24	1545.749	1545.750
0.31	1545.763	1545.764

Table 7: The force effect on the Bragg wave length, FWHM and power

Force (kg)	Bragg wave length (nm)	FWHM (pm)	Power (nW)
0.25	1545.601	169.455	2.33
0.50	1545.611	185.234	2.11
0.75	1545.656	291.743	1.53
1.00	1545.662	280.418	1.67

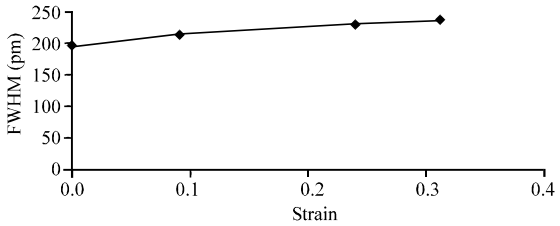

Fig. 11: The relation between mechanical effect (strain) and FWHM

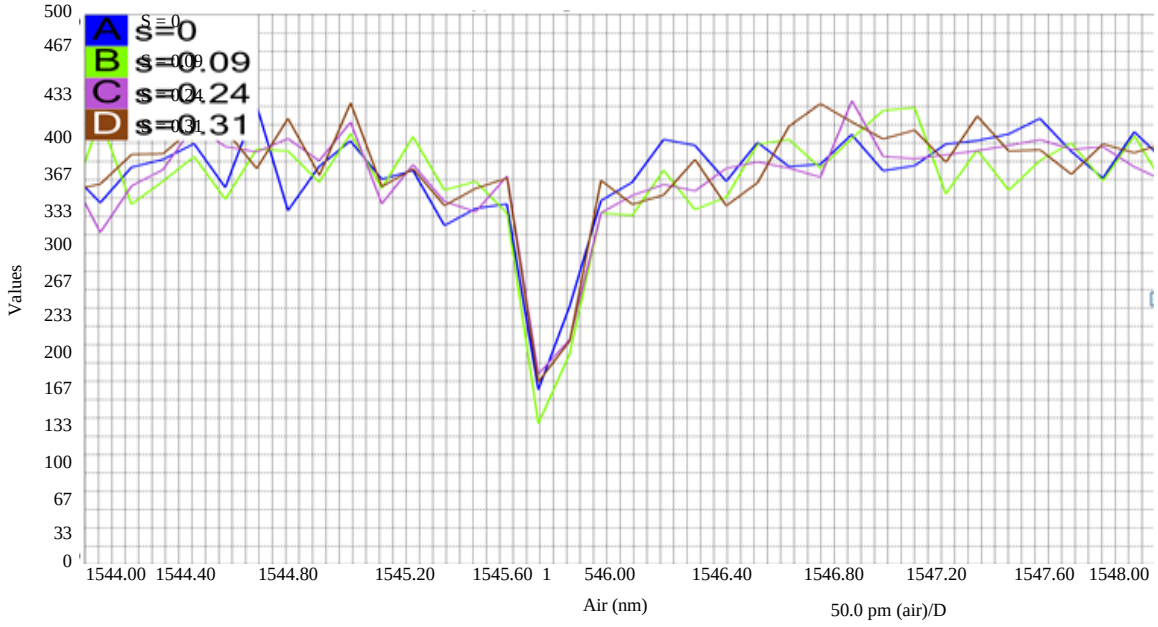

Fig 12: Transition spectrum of tunable optical notch FBG filter when applied strain on the second arm of homodyne MZI

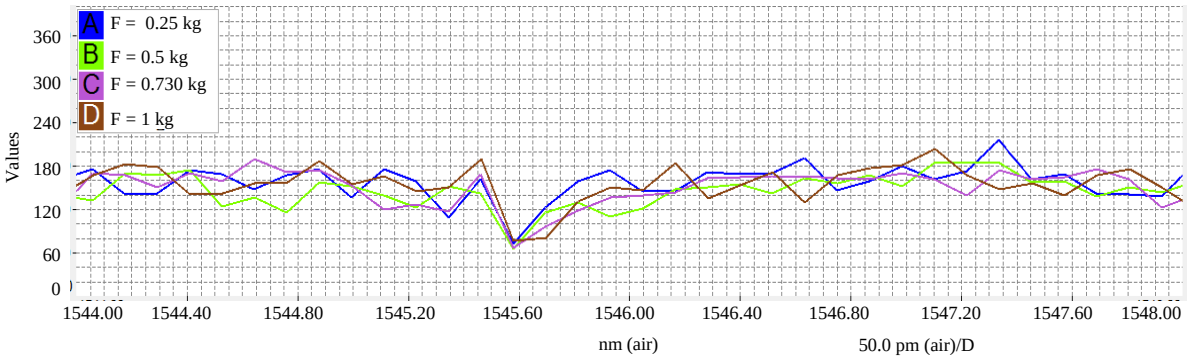

Fig. 13: Transition spectrum of tunable optical notch FBG filter when applied force on the second arm of homodyne MZI

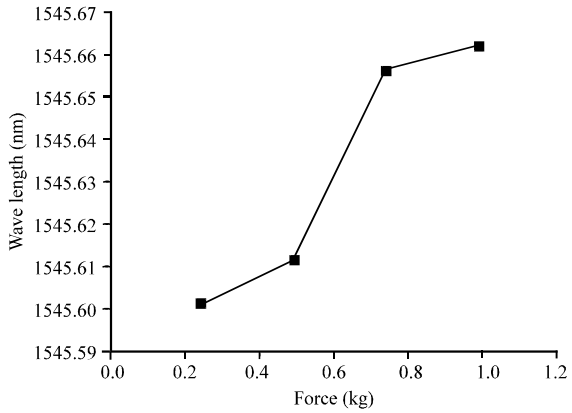

Fig. 14: The relation between the physical effect (Force) and wavelength

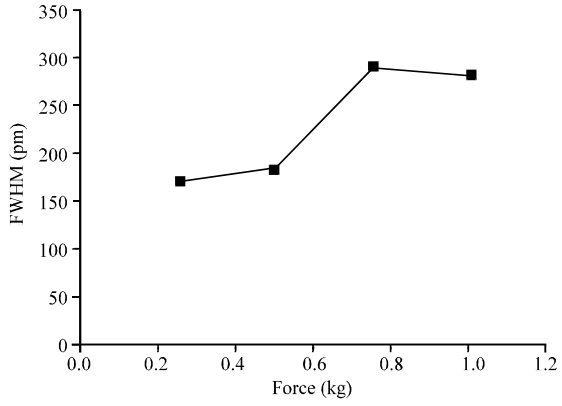

Fig. 15: The relation between physical effect (force) and FWHM

CONCLUSION

A generalized theory has been developed to analyze the implementation optical notch filter when the effects of the dispersion slope are relevant in the propagation of the optical signal along the optical delay line. The filter is based on homodyne MZI, illuminated with a broadband source and a fiber length used as dispersive element. When we applied physical and mechanical effect which are force and strain on the second arm of homodyne MZI, i.e. (effected arm) the length of the fiber is changed and then we obtainedpracticaly shifted in central wavelength λ_B (red shift) with range (1545.726-1545.764 nm), FWHM (197.529-238.081) pm and the power (12.1-11) nW and with force effect the range of λ_B = 1545.601-1545.662 nm, FWHM = (169.455-291.743) pm and power = 1.53-2.33 nW, In theoretical Optwave we obtained red shift with range (1545.766-1546.25) nm and this results different from practical because the practical results implemented at laboratory temperature and the optical fibers very sensitive to temperature, so, changed the refractive index of these fibers. The change in these parameters caused by strain and force effects will be effected on the phase shift of homodyne MZI. As a result that will be obtained tunability in the optical notch filter and it is equal (0.484) nm. The wavelength shift of the FBG can be used to measure tunable filter and the output is a convolution of both the spectrum of the tunable filter and that of the FBG, so, we use this type of MZI, i.e. (homodyne MZI).

REFERENCES

Allsop, T., R. Reeves, D.J. Webb, I. Bennion and R. Neal, 2002. A high sensitivity refractometer based upon a long period grating Mach-Zehnder interferometer. Rev. Sci. Instrum., 73: 1702-1705.

Anonymous, 2003. Encoded optical CDMA using superimposed fiber Bragg gratings. The Optical Society, Washington, DC, USA.

Chung, K.M., 2012. Advanced fibre Bragg grating and microfibre Bragg grating fabrication techniques. Ph.D Thesis, Hong Kong Polytechnic University, Hong Kong.

Jackson, D.A., A.D. Kersey, M. Corke and J.D.C. Jones, 1982. Pseudoheterodyne detection scheme for optical interferometers. Electron. Lett., 18: 1081-1083.

Lee, B.H., Y.H. Kim, K.S. Park, J.B. Eom and M.J. Kim *et al*., 2012. Interferometric fiber optic sensors. Sens., 12: 2467-2486.

Meera, J.P. and P.P. Anuradha, 2014. A survey paper of optical fiber sensor. Intl. J. Recent Innovation Trends Comput. Commun., 2: 2321-8169.

Mizunami, T., T.V. Djambova, T. Niiho and S. Gupta, 2000. Bragg gratings in multimode and few-mode optical fibers. J. Lightwave Technol., 18: 230-235.

Navruz, I. and N.F. Guler, 2008. A novel technique for optical dense comb filters using sampled fiber Bragg gratings. Opt. Fiber Technol., 14: 114-118.

Tan, Z., Y. Wang, W. Ren, Y. Liu and B. Li *et al*., 2009. Transmission system over 3000 km with dispersion compensated by chirped fiber Bragg gratings. Optik Intl. J. Light Electron. Opt., 120: 9-13.

Wu, Q., C. Yu, K. Wang, X. Wang and Z. Yu *et al*., 2005. New sampling-based design of simultaneous compensation of both dispersion and dispersion slope for multichannel fiber Bragg gratings. IEEE. Photonics Technol. Lett., 17: 381-383.